Perturbation Approach on MHD Flow through an Accelerated Vertical Porous Plate with Thermal Radiation

Kaleeswari. S[1] ,Mohanambal. B[2*]

[1]Assistant Professor, Department of Mathematics, Nallamuthu Gounder Mahalingam College, Pollachi Coimbatore, Tamil Nadu, India.
[2]Assistant Professor, Department of Mathematics, Akshaya College of Engineering and Technology, Kinathukadavu, Coimbatore, Tamil Nadu, India, Email: bmohanasri@gmail.com
[*]Corresponding Author

Received: 05.04.2024 Revised: 10.05.2024 Accepted: 24.05.2024

ABSTRACT
The article discusses a mathematical model of free convective flow in magnetohydrodynamics across an accelerating vertical porous plate with heat radiation. Analytical formulas for the fluid temperature and velocity are derived using a novel perturbation method. The resulting analytical formulas are used to investigate how fluid temperature and velocity are affected by the magnetic field, chemical reaction, and other pertinent flow aspects. The outcomes describes that there is a decrease in velocity and a temperature rise when the magnetic field parameters are increased. The temperature and velocity will both decrease when the stratification factor increases. The temperature profiles become smaller as one increases the radiation parameter.

Keywords: Thermal diffusion, MHD, Mixed convection, Porous medium, Nano-fluid, Stratified fluid, Unsteady flow.

INTRODUCTION

Agarwal et al. [1] investigated the MHD flow with a stretching sheet and porous medium and used similarity and transformation techniques to estimate the conclusion that enhancing the heat transfer using the Prandtl number. Another report [2] analyzed the muddled third-grade fluid with hafnium nanoparticles as a slippery wall flow and expressed that it has a convergent channel. They concluded that enhanced velocity profile by volumetric flow parameter. The report of Kumar et al. [3] and Ogunseye et al. [4] used the Lie similarity technique to transform the differential equation of electrical conducting fluid and heat transfer equation to solve through numerical methods and discussed the dynamic fluid behaviors.

Thenmozhiet. al. [5], described the mathematical model of analysis of the heat transfer system and the application of the heat transfer system in industrial machines, mass cloud data storage compartments, and electronic device refrigeration. Prameelaet. al. [6], investigation is to examine magnetohydrodynamic natural convective, mass, and heat transfer, performing non-Newtonian Casson fluid flow through an oscillating straight-up permeable plate with the existence of thermal diffusion. Shankar Goud et.al analyze the unsteady MHD flow via a porous medium past an accelerating vertical plate in a thermally stratified flow of fluid in the existence of viscous dissipation. Many Authors explored the numerous phases of the MHD fluid flow control viz. [7 – 12].

RaghunathKodiet. al. [13], investigate the magnetohydrodynamic (MHD) mixed convection flow for Maxwell nanofluid, which is debated in the context of a vertical cone containing porous material. In addition, variable thermal conductivity and Dufour's effects are considered. Ijaz and Ayub [14] examined the stratified flow of Maxwell nanofluid in the presence of activation energy. Mabood et al. [15] examine the Maxwell fluid model with variable thermal conductivity. The latter paper considered the swirling motion of the liquid in a rotating disk. Liu et al. [16] used the Fast method and convergence analysis for the magnetohydrodynamic flow and heat transfer of fractional Maxwell fluid. Akyildiz and Alshammari [17] have studied a new analysis of Galerkin Legendre spectral methods for coupled hyperbolic/parabolic systems arising in unsteady MHD flow of Maxwell fluid and numerical simulation. Several researchers have focused on Maxwell fluid flow analysis with various physical aspects applicable to a variety of situations [18 - 20].

Khadija Rafiqueet. al. [21], examine the impact of NP shape on the entropy production of a water-alumina nanofluid over a permeable MHD stretching sheet at quadratic velocities with viscous dissipation and

joule heating. Maxwell [22] discovered in the 19th century that it is possible to increase the thermal conductivity of a fluid by suspending several different substances, each of which has a stronger conductivity, for example, solid particles. This discovery was made possible by the fact that it is possible to increase the number of different substances that have a stronger conductivity.
In this study, Mandal et al. [23] analyze the entropy production of MHD bioconvective flow of Maxwell nanofluid consisting of gyrotactic microorganisms flowing across a radiatively inclined stretched cylinder. ThamizhSuganya et al. [24] obtained an analytical expression of the profiles of velocity and temperature and the analysis of the sensitivity of magnetohydrodynamic free convective flow in an inclined plate.

Mathematical formulation of the problem
A naturally convective and thermally radiative incompressible simple fourth-grade fluid is defined for the unsteady case model, and the fluid passes through a vertical infinite porous plate with a destructive chemical reaction and heat generation effect (Fig. 1).

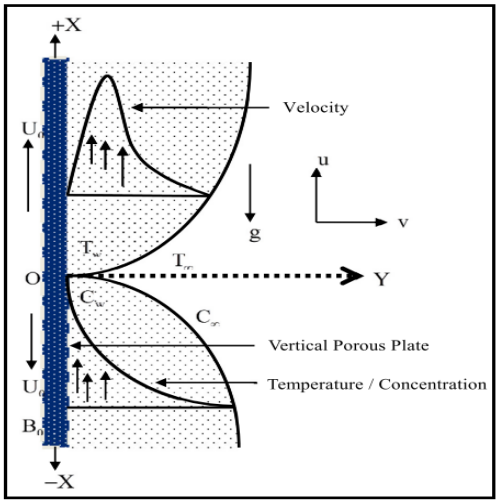

Fig 1. The physical configuration of the flow.

The resultant set of equations shows the flow shape (Fig. 1) and modal.

$$\frac{\partial u^*}{\partial t^*} = v\frac{\partial^2 u^*}{\partial y^{*2}} + g\beta(T^* - T_\infty^*) - \left(\frac{\sigma B_0^2}{\rho}\right)u^* - \frac{v}{K^*}u^* \tag{1}$$

$$\frac{\partial T^*}{\partial t^*} = \alpha\frac{\partial^2 T^*}{\partial y^{*2}} - \gamma u^* - \frac{\mu}{\partial C_p}\left(\frac{\sigma u^*}{\partial y^*}\right)^2 - \frac{1}{\partial C_p}\frac{\sigma q_r}{\partial y^*} \tag{2}$$

Where $\gamma = \frac{dT_\infty}{dz} + \frac{g}{C_p}$.

The term $\frac{dT_\infty}{dz}$ represent thermal stratification and $\frac{g}{C_p}$ represent pressure work
The proper conditions are:

$$\left.\begin{aligned} &t^* \le 0 : \forall y^* : u^* = 0, T^* = T_\infty^*, \\ &t^* > 0 : u^* = At^*, T^* = T_\omega^* \ at \ y^* = 0 \\ &u^* \to 0, T^* \to T_\infty^*, \ as \ y^* \to \infty \end{aligned}\right\} \tag{3}$$

WhereA(> 0) is defined as stable acceleration, the heat at the blocks can be denoted by T_ω^∞, and t^* be the time.
The following non-dimensional quantities are introduced:

$$y=\sqrt{\frac{A}{v}}y^*, u=u^*, t=At^*, K=\frac{K^*A}{v}, Gr=\frac{g\beta(T_\omega^*-T_\infty^*)}{A}, M=\frac{\sigma B_0^2}{\rho A}, S=\frac{\gamma}{A(T_\omega^*-T_\infty^*)},$$

$$\Pr=\frac{\mu C_p}{k}, \theta=\frac{T^*-T_\infty^*}{T_\omega^*-T_\infty^*}, \mu=\rho v, Ec=\frac{1}{C_p(T_\omega^*-T_\infty^*)}, R=\frac{k_e K}{4\sigma_s T_\infty^{*3}}. \quad (4)$$

It is possible to simplify Eqs. (1) and (2) using dimensionless values with steady-state conditions.

$$\frac{\partial^2 u}{\partial y^2}+Gr\theta-Mu-\frac{1}{K}u=0 \quad (5)$$

$$\frac{1}{\Pr}\left[1+\frac{4}{3R}\right]\frac{\partial^2\theta}{\partial y^2}+Su+Ec\left(\frac{\partial u}{\partial y}\right)^2=0 \quad (6)$$

The appropriate non-dimensional boundary conditions are:

$$u=0,\quad \theta=1,\quad at \qquad y=0 \quad (7)$$

$$u\to 0,\ \theta\to 0,\quad as\quad y\to\infty \quad (8)$$

All the symbols are defined in nomenclature. The mathematical statement of the problem is now complete and represents the solutions of Eqs. (5) & (6) subject to boundary conditions (7) & (8). For realistic engineering applications and the design of chemical engineering systems based on this type of boundary layer flow, the Skin friction and Nusselt number (Rate of heat transfer) are important physical parameters.

The non-dimensional form of the Skin-friction at the plate is stated by

$$\tau=\frac{\tau_\omega}{\rho V_0}\left(\frac{\partial u^*}{\partial y^*}\right)_{y^*=0}=-\left(\frac{\partial u}{\partial y}\right)_{y=0} \quad (9)$$

The heat transfer velocity, which is in the non-dimensional form in terms of the Nusselt number is specified by

$$Nu=\frac{x^*}{T_\omega^*-T_\infty^*}\left(\frac{\partial T^*}{\partial y^*}\right)_{y^*=0}=-\left(\frac{\partial\theta}{\partial y}\right)_{y=0} \quad (10)$$

Analytical solution by perturbation method

The non-linear momentum and energy Eqs. (5) and (6) can be solved by using the implicit perturbation approach of the Crank & Nicolson model after the appropriate initial and boundary constraints (7) & (8) have been set up. Homotopy perturbation method (HPM) is an analytical technique for resolving a set of real-world engineering issues from many domains.

To rewrite the given differential equations as follows,

$$\frac{d^2u}{dy^2}+Gr\theta-\left(M+\frac{1}{K}\right)u=0 \quad (11)$$

$$\frac{d^2\theta}{dy^2}+\frac{3R\cdot\Pr}{3R+4}\cdot Su+\frac{3R\cdot\Pr}{3R+4}\cdot Ec\left(\frac{du}{dy}\right)^2-k_1\theta+k_1\theta=0 \quad (12)$$

The boundary conditions (11) and (12) take the dimensionless form with the following Eqs. (13) and (14):

$$u=0,\quad \theta=1,\quad at \qquad y=0 \quad (13)$$

$$u\to 0,\ \theta\to 0,\quad as\quad y\to\infty \quad (14)$$

The analytical outcomes are preceded by the implementation of the perturbation technique.

$$u=u_0+pu_1+p^2u_2+\ldots \quad (15)$$

$$\theta = \theta_0 + p\theta_1 + p^2\theta_2 + \ldots \tag{16}$$

After replacing Eq. (15) & (16) with Eqs. (11) & (12) and Construct the homotopy perturbation techniques as follows:

$$(1-p)\left[\frac{d^2u}{dy^2} - \left(M + \frac{1}{K}\right)u\right] + p\left[\frac{d^2u}{dy^2} + Gr\theta - \left(M + \frac{1}{K}\right)u\right] = 0 \tag{17}$$

$$(1-p)\left[\frac{d^2\theta}{dy^2} - k_1\theta\right] + p\left[\frac{d^2\theta}{dy^2} + \frac{3R\cdot \Pr}{3R+4}\cdot Su + \frac{3R\cdot \Pr}{3R+4}\cdot Ec\left(\frac{du}{dy}\right)^2 - k_1\theta + k_1\theta\right] = 0 \tag{18}$$

where most important denotes common place differentiation with high opinion to y. The consequent border line circumstances can be on paper as and substituting equations (15) & (16) into equations (17) & (18), and equate the terms with the identical powers of p^0 & p^1, we obtain

$$p^0 : \frac{d^2u_0}{dy^2} - \left(M + \frac{1}{K}\right)u_0 = 0 \tag{19}$$

$$p^1 := \frac{d^2u_1}{dy^2} - \left(M + \frac{1}{K}\right)u_1 + Gr\theta_0 = 0 \tag{20}$$

$$p^0 : \frac{d^2\theta_0}{dy^2} - k_1\theta_0 = 0 \tag{21}$$

$$p^1 : \frac{d^2\theta_1}{dy^2} - k_1\theta_1 + k_1\theta_0 + \frac{3R\cdot \Pr}{3R+4}\cdot Su_0 + \frac{3R\cdot \Pr}{3R+4}\cdot Ec\left(\frac{du_0}{dy}\right)^2 = 0 \tag{22}$$

The corresponding physical dimensionless conditions are:

$$u_0 = a, u_1 = -a, \theta_0 = 1, \theta_1 = 0, \quad at \qquad y = 0 \tag{23}$$

$$u_0 \to 0, u_1 \to 0, \theta_0 \to 0, \theta_1 \to 0 \qquad as \quad y \to \infty \tag{24}$$

The outcomes of Eqs. (19)–(22) with Eq. (23) & (24) results into following Eqs. (25)-(28):

$$u_0 = ae^{-\sqrt{M+\frac{1}{K}}\,y} \tag{25}$$

$$\theta_0 = e^{-\sqrt{k_1}y} \tag{26}$$

$$u_1 = \frac{Gr}{\left(M + \frac{1}{K} - k_1\right)}\left(e^{-\sqrt{k_1}y} - e^{-\sqrt{M+\frac{1}{K}}\,y}\right) - ae^{-\sqrt{M+\frac{1}{K}}\,y} \tag{27}$$

$$\theta_1 = \frac{y\cdot\sqrt{k_1}\cdot e^{-\sqrt{k_1}y}}{2} + \frac{3R\cdot \Pr\cdot S}{(3R+4)(M+\frac{1}{K}-k_1)}\left[e^{-\sqrt{k_1}y} - e^{-\sqrt{M+\frac{1}{K}}\,y}\right]$$
$$+ \frac{3R\cdot Ec\cdot \Pr\cdot a^2\cdot M + \frac{1}{K}}{(3R+4)(4M+\frac{4}{K}-k_1)}\left[e^{-\sqrt{k_1}y} - e^{-2\sqrt{M+\frac{1}{K}}\,y}\right] \tag{28}$$

The solution of problem is presented in Eqs. (23)–(31)

$$u = u_0 + u_1 \qquad and \qquad \theta = \theta_0 + \theta_1 \tag{29}$$

$$u = \frac{Gr}{\left(M + \frac{1}{K} - k_1\right)}\left(e^{-\sqrt{k_1}y} - e^{-\sqrt{M+\frac{1}{K}}y}\right) \tag{30}$$

$$\theta = e^{-\sqrt{k_1}y} + \frac{y\cdot\sqrt{k_1}\cdot e^{-\sqrt{k_1}y}}{2} + \frac{3R\cdot \Pr\cdot S}{(3R+4)(M+\frac{1}{K}-k_1)}\left[e^{-\sqrt{k_1}y} - e^{-\sqrt{M+\frac{1}{K}}y}\right]$$

$$+\frac{3R\cdot Ec\cdot \Pr\cdot a^2\cdot M+\frac{1}{K}}{(3R+4)(4M+\frac{4}{K}-k_1)}\left[e^{-\sqrt{k_1}y} - e^{-2\sqrt{M+\frac{1}{K}}y}\right] \tag{31}$$

In boundary layers, physical parameters such as the skin friction coefficient and the Nusselt number of heat transfer the flow. The non-dimensional form of the Skin friction at the plate is given by,

$$\tau = \frac{\tau_\omega}{\rho V_0}\left(\frac{\partial u^*}{\partial y^*}\right)_{y^*=0} = -\left(\frac{\partial u}{\partial y}\right)_{y=0}$$

$$\tau = -\frac{Gr\cdot K\cdot\left(\sqrt{\frac{M\cdot K+1}{K}} - \sqrt{k_1}\right)}{1+(M-k_1)\cdot K} \tag{32}$$

The heat transfer velocity, which is in the non-dimensional form in terms of the Nusselt number is specified by,

$$Nu = \frac{x^*}{T_\omega^* - T_\infty^*}\left(\frac{\partial T^*}{\partial y^*}\right)_{y^*=0} = -\left(\frac{\partial \theta}{\partial y}\right)_{y=0}$$

$$Nu = \frac{\sqrt{k_1}}{2} - \frac{3R\cdot \Pr\cdot S\cdot\left(M+\frac{1}{K}-\sqrt{k_1}\right)}{(3R+4)\left(M+\frac{1}{K}-k_1\right)} - \frac{3R\cdot Ec\cdot \Pr\cdot a^2\cdot M+\frac{1}{K}\cdot\left(2\sqrt{M+\frac{1}{K}}-\sqrt{k_1}\right)}{(3R+4)\left(4M+\frac{4}{K}-k_1\right)} \tag{33}$$

RESULTS AND DISCUSSION

This section of the research work deals with the detailed overview of the key analytical findings and physical interpretation of different emerging parameters such as Gr, Pr, M, Ec, K, k1, R, S, a, and Nu are the Grashof number, Prandtl number, magnetic field parameter, Eckert number, parameter of temperature, permeability parameter, heat source parameter, parameter of velocity, skin friction and Nusselt number respectively. The behavior of the velocity profile u(y) temperature profile θ(y) and the effects of the mentioned physical parameters are deliberated as well as graphical illustration is made via MAPLE.

Figs. (2.a) display the velocity field for varying quantities of the Grashof number. It seems that when Gr grows, the heat field diminishes and the velocity field increases. The Grashof number Gr represents the relationship between the thermal attraction and the boundary-layer viscous hydrodynamic force. There is a velocity increase consistent with the expected result of the greater thermal stability force. Falling Gr values here indicate that the plate is cooling. In addition, the peak values of the velocity near the porous plate rise abruptly as Gr increases and then gradually decrease to the free stream velocity.

The properties of the speed for analytical values of the parameter for permeability(K) are seen in Figs. (2.b) respectively. The velocity of the fluid rises, when the values of K are increased. Physically, a destructive chemical reaction occurs with more disturbances which develops the molecular motion and upsurges the heat transport phenomena, as a result, the concentric profiles diminish.

Fig. (2.c) illustrates the skin friction profiles for the increment of the magnetic parameter (M). The fields of rising data of M because the imposed magnetic field tends to decelerate the fluid flows and hence the surface friction force declines. For the increase of higher order material parameters, elastic

characteristics deformation leads to the changes of shape or size of fluid due to an applied force or transformation of heat. For the increase of viscoelastic property, the momentum boundary layer thickness becomes more conservator with the plate, for this reason, velocity profiles decrease. With the rise of higher-order material parameters, the viscoelasticity property enhances the molecular particle gathering and temperature absorption rate increase. As a result, the fluid region temperature increases for higher-order material parameters. Fig. (2.d) depicts the drag force effect on fluid flow and decreases the velocity profiles with the increase of the temperature parameter (k_1).

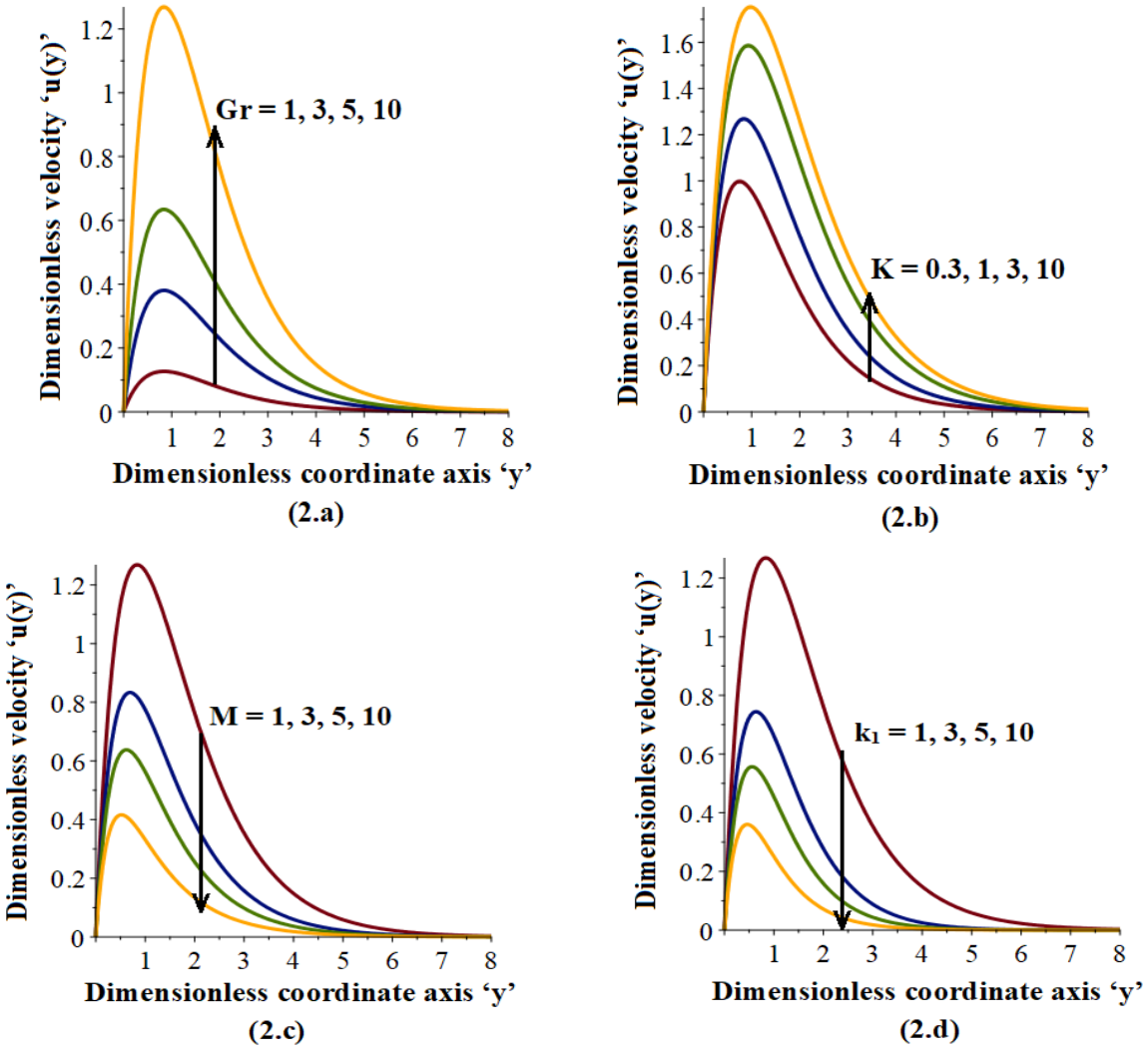

Figure 2: Dimensionless velocity profile 'u(y)' versus dimensionless coordinate axis 'y' for fixed experimental values of parameters.

The effects of the parameters on the temperature distribution are displayed by the radiation parameter (R), permeability parameter (K), and magnetic parameter (M). The graph shows that temperature curves become smaller in Figs. (3.a) through (3.c) when the Radiation parameter increases. The drag force effect on fluid flow is seen in Fig. (3.d), where an increase in the temperature parameter (k1) results in a decrease in the temperature profiles.

In Fig. (3.e), it is noticed that how the Prandtl number influence the temperature distributions. This chartrepresents that a fall in the temperature of the fluidtake place as Prdecreases. The Pr values could be definite as the proportion of kinematic consistency to thermal diffusivity. The impact that Ec has on temperature is seen in Fig. (3.f). The heat that is produced as a consequence of friction heating contributes to a rise in the temperature of the wall caused by Ec.

The temperature variations caused by varying the stratification parameter (S) and velocity parameter (a) are shown in Fig. (3.g) & Fig. (3.h), respectively. As the stratification factor rises, the temperature increases.

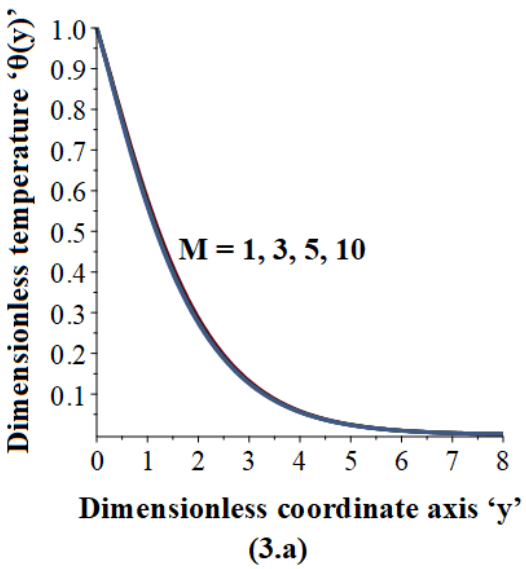

(3.a)

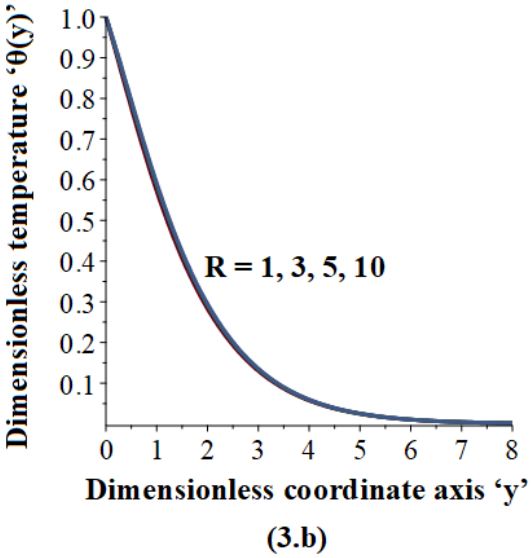

(3.b)

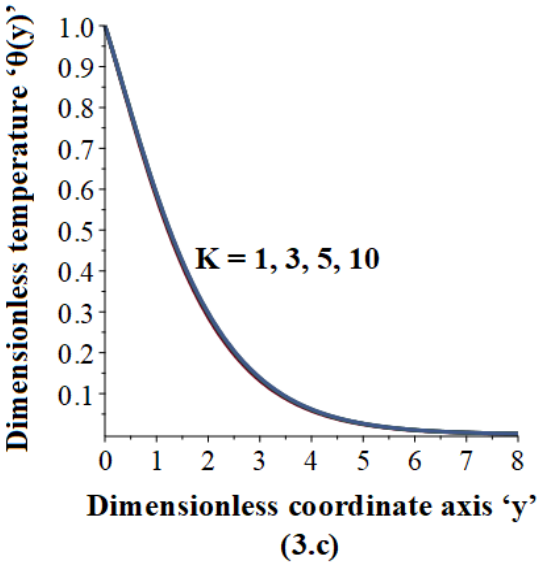

(3.c)

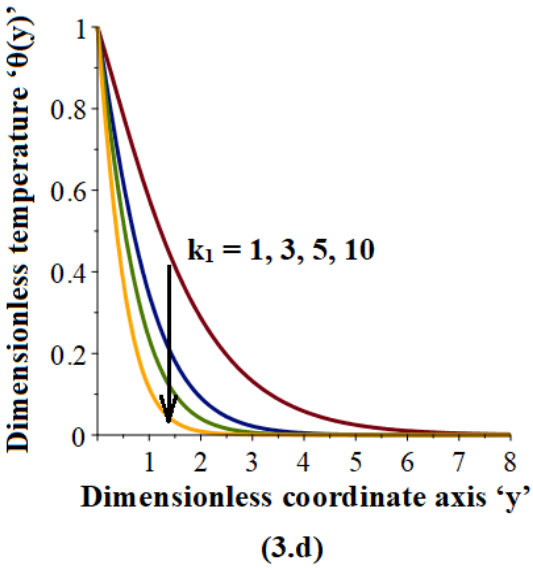

(3.d)

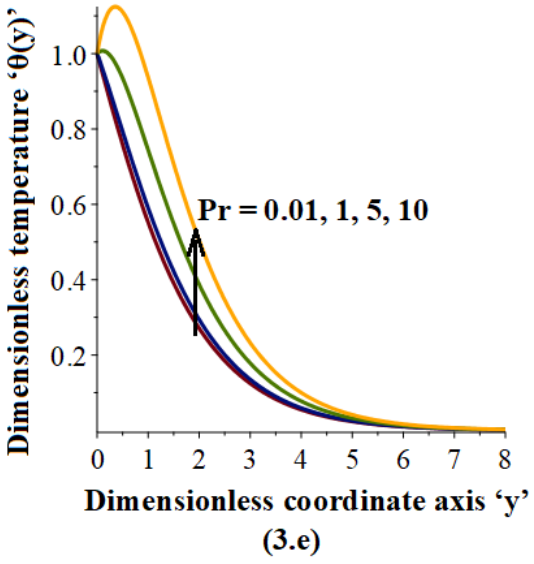

(3.e)

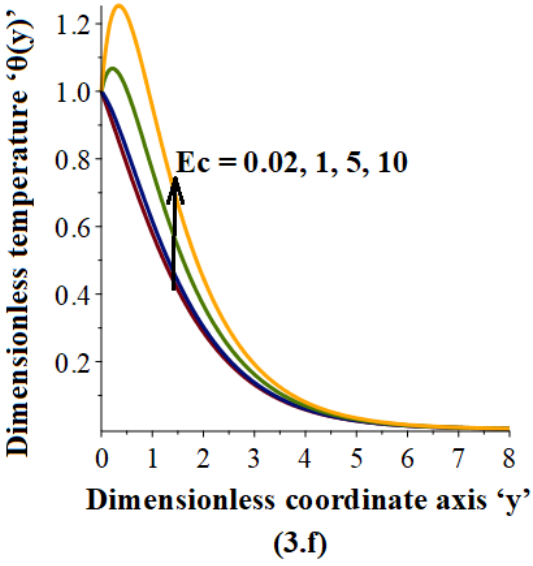

(3.f)

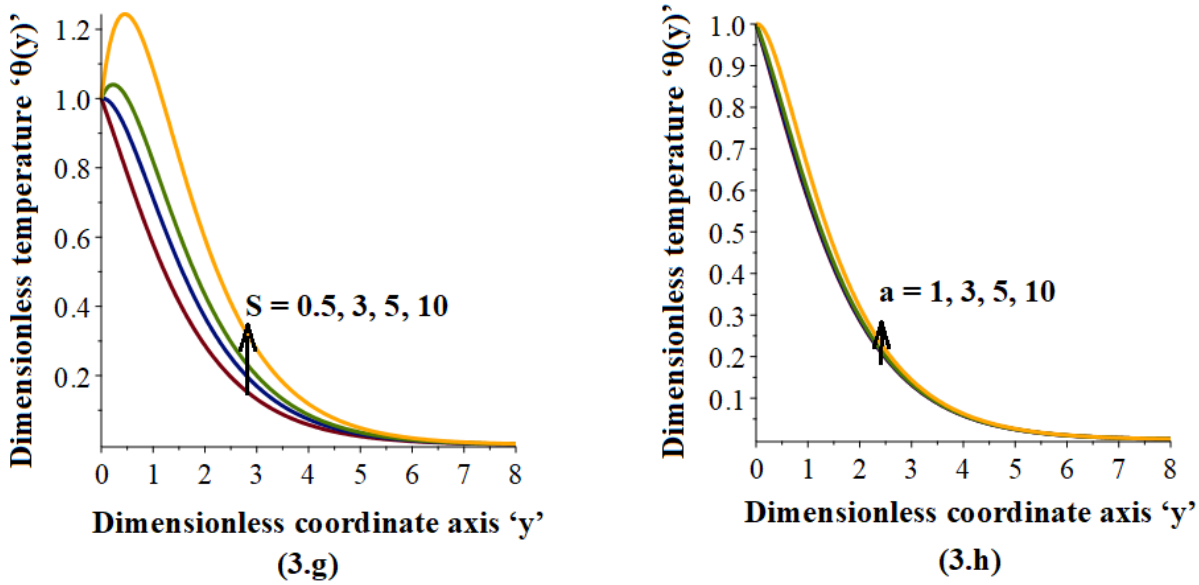

Figure 3: Dimensionless temperature profile 'θ(y)' versus dimensionless coordinate axis 'y' for fixed experimental values of parameters.

CONCLUSION

We have examined analytically the MHD boundary layer flow problem of the thermally stratified fluid with viscus dissipation flows over a permeable medium past an accelerating vertical plate. To put analytical solutions into practice, the perturbation approach is utilized. The results are displayed using graphs and tabular data presentations. This article looks into a number of the many physical elements that affect the fluid's flow regime.

As the magnetic parameter rises, we can see that the velocity profile reduces in the flow region. Thus, we conclude that we can control the velocity field by introducing a magnetic field, but the reversed phenomenon is noted by increasing the permeability parameter value. As M and S grow, the width of the momentum boundary layer decreases, but it rises as Gr, K, and Ec. The variables M, and Ec, increase when the temperature rises, whereas Gr, K, S, and Pr all increase as the temperature falls. When the values of M, S, Pr& R are raised, the values of friction also rise. Nusselt number distribution rises due to the enhancement in thermal radiation. In streamlined and isothermal lines, higher thermal radiation levels increase the thickness of the thermal and momentum boundary layers. As an outcome, this approach is an effective mathematical tool for resolving both linear and nonlinear differential equations.

REFERENCES

[1] P. Agarwal, P.K. Daheech, R.N. Jat, M. Bohra, K.S. Nisar, K.S. Khan, Lie similarity analysis of MHD flow past a stretching surface embedded in the porous medium along with imposed heat source/sink and variable viscosity, J. Mater. Res. Technol. 9 (5) (2020) 10045–10053.

[2] M. Nazeer, Development and theoretical analysis of slippery walls flow of third-grade fluid through the convergent symmetric channel, Waves Random Complex Media 24 (2022) 1–20.

[3] H.A. Ogunseye, S.O. Salawu, S.D. Oloniiju, M.T. Akolade, Y.O. Tijani, R. Mustapha, P. Sibanda, MHD Powell–Eyringnanofluid motion with the convective surface condition and Dufour–Soret impact past a vertical plate: lie group analysis, Partial Differ. Equ. Appl. Math. 6 (2022), 100459. Dec 1.

[4] T.M. Kumar, N.A. Shah, V. Nagendramma, P. Durgaprasad, N. Sivakumar, B. M. Rao, C.S. Raju, S.J. Yook, Linear regression of triple diffusive and dual slip flow using lie group transformation with and without hydro-magnetic flow, AIMS Math. 8 (3) (2023) 5950–5979.

[5] D Thenmozhi , M. EswaraRao, RLV. Renuka Devi, Ch. Nagalakshmi, Analysis of Jeffrey fluid on MHD flow with stretching – porous sheets of heat transfer system, Forces in Mechanics, 2023, 1-7.

[6] M. Prameela, K. Gangadhar, G. Jithender Reddy, MHD free convective non-Newtonian Casson fluid flow over an oscillating vertical plate, Partial Differential Equations in Applied Mathematics, 5(2022)100366.

[7] B. Shankar Goud, PudhariSrilatha, D. Mahendar, ThadakamallaSrinivasulu, YanalaDharmendar Reddy, Thermal radiation effect on thermostatically stratified MHD fluid flow through an accelerated vertical porous plate with viscous dissipation impact, Partial Differential Equations in Applied Mathematics, 7 (2023) 100488.

[8] Shankar Goud B. Thermal radiation influences on MHD stagnation point stream over a stretching sheet with slip boundary conditions. Int J ThermofluidSci Technol. 2020;7(2):1–11.
[9] Kenneth AsogwaKanayo, Shankar Goud B, Ali Shah Nehad, Se-JinYook. Rheology of electron magnetohydrodynamic tangent hyperbolic nanofluid over a stretching Riga surface featuring Dufour effect and activation energy. Sci Rep. 2022:12. http://dx.doi.org/10.1038/s41598-022-18998-914602.
[10] Akram M, Jamshed W, Shankar BG, et al. Irregular heat source impact on carreaunanofluid flowing via exponential expanding cylinder: A thermal case study. Case Stud Therm Eng. 2022;36:102171:1-14.
[11] Shankar BG, Dharmendar Reddy Y, Mishra SR. Joule heating and thermal radiation impact on MHD boundary layer nanofluid flow along an exponentially stretching surface with the thermally stratified medium. ProcInstMechEng, Part N: J NanomaterNanoengNanosyst. 2022. http://dx.doi.org/10.1177/ 23977914221100961.
[12] Asogwa KK, Shankar BG, Yanala, Reddy Dharmendar. Non-Newtonian electromagnetic fluid flow through a slanted parabolic started Riga surface with ramped energy. Heat Transfer. 2022;51(6):4833–6026.
[13] RaghunathKodi, CharankumarGanteda, AbhishekDasore, M. Logesh Kumar, G. Laxmaiah, MohdAbulHasan, Saiful Islam, Abdul Razak, Influence of MHD mixed convection flow for maxwellnanofluid through a vertical cone with porous material in the existence of variable heat conductivity and diffusion, Case Studies in Thermal Engineering, 44 (2023) 102875.
[14] M. Ijaz, M. Ayub, Nonlinear convective stratified flow of Maxwell nanofluid with activation energy, Heliyon 5 (2019), e01121.
[15] F. Mabood, A. Rauf, B.C. Prasannakumara, M. Izadi, S.A. Shehzad, Impacts of Stefan blowing and mass convention on the flow of Maxwell nanofluid of variable thermal conductivity about a rotating disk, Chin. J. Phys. 71 (2021) 260–272
[16] Y. Liu, X. Chi, H. Xu, X. Jiang, Fast method and convergence analysis for the magnetohydrodynamic flow and heat transfer of fractional Maxwell fluid, Appl. Math. Comput. 430 (2022), 127255.
[17] F.T. Akyildiz, F. Alshammari, A new analysis of Galerkin Legendre spectral methods for coupled hyperbolic/parabolic system arising in unsteady MHD flow of Maxwell fluid and numerical simulation, Appl. Numer. Math. 176 (2022) 83–103.
[18] Y. Zhang, J. Gao, Y. Bai, Q. Wang, D. Sun, X. Sun, B. Lv, Numerical simulation of the fractional Maxwell fluid flow in the locally narrow artery, Comput. Methods Biomech. Biomed. Eng. (2022) 1–16.
[19] D.J. Samuel, Numerical investigations of thermal radiation and activation energy imparts on chemically reactive Maxwell fluid flow over an exothermal stretching sheet in a porous medium, Int. J. Appl. Comput. Math. 8 (2022) 148.
[20] D.J. Samuel, B.I. Olajuwon, Insight into the effects of thermal radiation and Ohmic heating on chemically reactive Maxwell fluid subject to Lorentz force and buoyancy force, J. Niger. Math. Soc. 41 (2022) 27–48.
[21] Khadija Rafique, ZafarMahmood, Haifa Alqahtani, Sayed M Eldin, Various nanoparticle shapes and quadratic velocity impacts on entropy generation and MHD flow over a stretching sheet with joule heating, Alexandria Engineering Journal, 2023, 71, 147-159.
[22] J. C. Maxwell, A treatise on electricity and magnetism, vol. 1. Clarendon Press, 1873.
[23] M.K. Nayak, S. Shaw, M.I. Khan, O.D. Makinde, Y.-M. Chu, S.U. Khan, Interfacial layer and shape effects of modified Hamilton's Crosser model in entropy optimized Darcy Forchheimer flow, Alexandria Eng. J. 60 (4) (2021) 4067–4083.
[24] S. ThamizhSuganya, P. Balaganesan, L. Rajendran, Marwan Abukhaled, European journal of pure and applied mathematics, Analytical discussion and sensitivity analysis of parameters of magnetohydrodynamic free convective flow in an inclined plate, 13, 3, 2020, 631-644.